Comprehensive prediction method of road friction for vehicle dynamics control

6 authors, including:

Liang Li
Tsinghua University
155 PUBLICATIONS   **5,176** CITATIONS

SEE PROFILE

Jinglin Song
Philippine Women's University
131 PUBLICATIONS   **1,448** CITATIONS

SEE PROFILE

Comprehensive tire–road friction coefficient estimation based on signal fusion method under complex maneuvering operations

L. Li [a,*], K. Yang [a,b], G. Jia [a], X. Ran [a], J. Song [a], Z.-Q. Han [b]

[a] State Key Laboratory of Automotive Safety and Energy, Department of Automotive Engineering, Tsinghua University, Beijing, People's Republic of China
[b] Department of Automobile Engineering, Yanshan University, Hebei 066001, People's Republic of China

ARTICLE INFO

ABSTRACT

The accurate estimation of the tire–road friction coefficient plays a significant role in the vehicle dynamics control. The estimation method should be timely and reliable for the controlling requirements, which means the contact friction characteristics between the tire and the road should be recognized before the interference to ensure the safety of the driver and passengers from drifting and losing control. In addition, the estimation method should be stable and feasible for complex maneuvering operations to guarantee the control performance as well. A signal fusion method combining the available signals to estimate the road friction is suggested in this paper on the basis of the estimated ones of braking, driving and steering conditions individually. Through the input characteristics and the states of the vehicle and tires from sensors the maneuvering condition may be recognized, by which the certainty factors of the friction of the three conditions mentioned above may be obtained correspondingly, and then the comprehensive road friction may be calculated. Experimental vehicle tests validate the effectiveness of the proposed method through complex maneuvering operations; the estimated road friction coefficient based on the signal fusion method is relatively timely and accurate to satisfy the control demands.

© 2014 Elsevier Ltd. All rights reserved.

1. Introduction

The vehicle dynamics control systems, such as the anti-lock braking system (ABS), the traction control system (TCS), and the active yaw control system (AYC), have been equipped extensively in automotive industry nowadays to keep the stability of the suspension systems within limit conditions, which plays an important role in vehicle stability and ride comfort [1–4]. They work well only with the tire forces within the friction limit, which means knowledge of the tire–road friction may improve the performance of the systems [5], and for some control methods, the tire–road friction coefficient is the key state to the control accuracy. Thus the tire–road friction should be estimated accurately and robustly to acquire a relatively ideal controlling effect subjectively and objectively, which may guarantee the stability and accuracy of the control algorithm. An excellent review about the friction estimation method could be found in [6,7].

Various estimation methods of the road friction have been developed and improved since its importance is noticed to vehicle dynamics control. Generally speaking they are mainly divided into cause-based and effect-based approaches, which focus on the aspects that affect the road friction and the effects on the vehicle or the tire due to the change of the road friction [8–10]. Specifically Yamazaki estimated the road friction using an analytical approach based on a brush type tire model in real time, and tested indoors with a tire testing machine [11]. Carcaterra presented a procedure which can extract the tire–road contact kinematic parameter from time history of internal strain of the rolling tire based on the relationships between the measured strain and the area slip ratio using the tire dynamics model to identify the tire–road grip forces, and validated the algorithm with numerical simulations [12]. However the experimental ground tests were not conducted, which are significant for the validation of the robustness of the algorithm.

Lee used traction forces, a brake gain estimator and a normal force observer to estimate the road friction based on the relationship between the wheel slip ratio and the friction coefficient [13]. Rajamani proposed using observers to obtain the slip ratio and longitudinal tire force [14]; then a recursive least-square parameter identification formulation was used to identify the road friction. Hahn proposed an algorithm based on measurements related to lateral dynamics of the vehicle [15]. The estimation methods mentioned above realized experimental tests but this is just to the simple conditions with braking or driving only, such as those estimated for ABS, TCS or AYC separately, without considering the complex maneuvering operations. Besides, Hahn et al. [15] utilized an extra differential global positioning system (DGPS) and a gyroscope to identify the tire–road friction.

Hong estimated the road friction based on tire lateral deflection by determining the tire–road contact patch firstly [16], then filtering the lateral acceleration profile using the contact patch, and calculating the lateral force and aligning moment at last. Ray applied the Extended Kalman–Bucy Filter to estimate the states and tire force [17], then compared to those resulting from a nominal analytic tire model, and finally the Bayesian hypothesis selection was used to obtain the road friction. The algorithms are verified to be accurate enough through simulations and tests, but also too complex; the heavy computation becomes a burden to the micro-controller of the vehicle electric control unit, which may decrease the efficiency.

To summarize the research about the estimation of the tire–road friction has been developed from simulation only of ground tests, and different algorithms are proved to be effective. However, the proposed problems still exist. The separate estimation method for ABS, TCS and AYC and the complicated computation may make the performance not applicable and efficient enough.

According to the existing problems, a comprehensive estimation based on fusing the available signals which are the road frictions estimated by the wheels and the vehicle might be a useful method. The signal fusion method is discussed in [18,19]. The road frictions for different maneuvering conditions, such as, a high-intensity braking condition to the four wheels, a strong-power driving condition to the driving wheels and a sudden steering condition to the vehicle, might be estimated using simple but effective methods, which are described in detail in the following parts; then the weight of the estimated individual road friction might be set according to the longitudinal and lateral accelerations, the slip ratios and wheel slip angles, which results in a comprehensive estimated value of the road friction under complex operations.

The proposed signal fusion method overcomes the inapplicability of the separable estimation method for each system under complex maneuvering conditions, which may guarantee the control robustness. Besides, it can also make the estimation value much more accurate by utilizing the individual estimated friction of the ABS, TCS and AYC systems. This paper is organized as follows. The related models such as a 3DOF vehicle model, the Magic Formula tire model and the brake pressure estimation model are described in Section 2. In Section 3 the signal fusion method is proposed, including the confirmation of the certainty factors of the individual road frictions and the comprehensive one finally. Section 4 discusses the estimation methods for ABS runs, TCS runs, and AYC runs in Section 4.1, Section 4.2 and Section 4.3 respectively. The experimental test results on different roads are listed in Section 5.

2. Related models

2.1. Vehicle model

In order to present the dynamics characteristic a simple 3 DOF vehicle model is illustrated in Fig. 1, considering the longitudinal, lateral and yaw motions, and the related equations of the model are expressed as follows: The equation of the longitudinal motion is

$$m(\dot{V}_x - V_y\dot{\varphi}) = (F_{x11} + F_{x12})\cos\ \delta - (F_{y11} + F_{y12})\sin\ \delta + F_{x21} + F_{x22} \tag{1}$$

The equation of the lateral motion is

$$m(\dot{V}_y + V_x\dot{\varphi}) = (F_{x11} + F_{x12})\sin\ \delta + (F_{y11} + F_{y12})\cos\ \delta + F_{y21} + F_{y22} \tag{2}$$

and the equation of the yaw motion is

$$I_z\dot{\varphi} = (F_{y11} + F_{y12})a\ \cos\ \delta + (F_{y11} - F_{y12})b\ \sin\ \delta - (F_{y21} + F_{y22})b$$
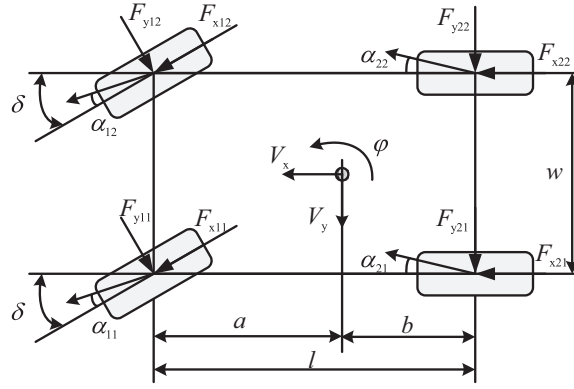$$- (F_{x11} + F_{x12})a\ \sin\ \delta - (F_{x11} - F_{x12})\frac{w}{2}\cos\ \delta - (F_{x21} - F_{x22})\frac{w}{2} \tag{3}$$

Fig. 1. The 3 DOF vehicle model.

Table 1
Tire's parameters (Michelin® MXV8 205/55R16 91V).

a_0	a_1	a_2	a_3	a_4	a_5	a_6	b_0
1.6	−34	1250	2320	12.8	0.0053	0.1925	1.55
b_1	b_2	b_3	b_4	b_5	b_6	b_7	b_8
0	1000	60	300	0.17	0	0	0.2

where m is the vehicle mass, V_x and V_y are the longitudinal and lateral velocities, $\dot{\varphi}$ is the yaw rate of the vehicle, F_{xij} and F_{yij} are the longitudinal and lateral forces of the four wheels, where ij of 11, 12, 21, 22 represents the front left, front right, rear left and rear right wheel respectively, δ is the steering angle of the front wheels, I_z is the inertia moment about vertical axis, a and b are the distances of the gravity centre to the front and rear axles, l is the wheelbase, and w is the track width of the vehicle.

2.2. The tire model

To reflect the transient characteristic of the tire in critical region, the Magic Formula (MF) as a nonlinear tire model is used in this paper to show the combined slip condition which a tire usually enters into the formula can be shown as

$$y(x) = D \sin \{C \arctan[Bx(1-E) + E \arctan(Bx)]\} \tag{4}$$

where $y(x)$ may be the longitudinal force, lateral force or aligning torque, and correspondingly x is the slip ratio λ (driving or braking conditions) or wheel slip angle α. D is the peak factor, C is the shape factor, B is the stiffness factor, and E is the curvature factor; these factors can be expressed as follows for longitudinal force:

$$\begin{cases} C = b_0 \\ D = b_1 F_z^2 + b_2 F_z \\ B = \frac{b_3 F_z^2 + b_4 F_z}{CD e^{b_5 F_z}} \\ E = b_6 F_z^2 + b_7 F_z + b_8 \end{cases} \tag{5}$$

while for lateral force, they are

$$\begin{cases} C = a_0 \\ D = a_1 F_z^2 + a_2 F_z \\ B = \frac{a_3 \sin [2\arctan(F_z/a_4)]}{CD} \\ E = a_5 F_z + a_6 \end{cases} \tag{6}$$

where F_z is the vertical load of each wheel; the parameters a_n and b_n may be derived from experiments, the values of which are listed in Table 1.
The slip ratio can be calculated by the equations below:

$$\lambda = \begin{cases} \frac{V_x - \omega R}{V_x} & V_x \geq \omega R \\ \frac{\omega R - V_x}{\omega R} & V_x < \omega R \end{cases} \tag{7}$$

where ω is the angular velocity of the rotated wheel, R is the wheel radius, and the longitudinal velocity V_x may be obtained by [20,21].

The wheel slip angles can be calculated as

$$\alpha_1 = \beta + \frac{a\dot{\varphi}}{V_x} - \delta \tag{8}$$

$$\alpha_2 = \beta - \frac{b\dot{\varphi}}{V_x} \tag{9}$$

where α_1 and α_2 are the front and rear wheel slip angles, respectively assuming that the two front wheel slip angles and the rear ones are the same. β is the vehicle slip angle, which may be obtained using the Extended Kalman Filter (EKF) method; also there is another way to estimate the slip angle through the integrated Kalman filter (IKF) [21] or the neural networks [22]. Here the variable structure EKF (VSEKF) with a feedback and damping item, brought forward by the author, might be adapted to observe the slip angle [23].

As for the vertical load of each wheel, since the body roll and pitch motions have considerable effects, the load transfer should be taken into account, thus, the load on four wheels with acceleration or deceleration during steering may be expressed as [24]

$$F_z = F_{z0} \pm \sigma_1 a_x \pm \sigma_2 a_y \tag{10}$$

where F_z and F_{z0} are the vertical load and its static value of each wheel, respectively, a_x and a_y are the longitudinal and lateral accelerations; σ_1 and σ_2 are the coefficients related to the accelerations.

The longitudinal and lateral forces under combined driving/braking–steering conditions should satisfy the adhesion ellipse, so the forces obtained from MF should be corrected as

$$F_x = \frac{|\sigma_x|}{\sigma} y(x), \quad F_y = \frac{|\sigma_y|}{\sigma} y(x) \tag{11}$$

$$\sigma = \sqrt{\sigma_x^2 + \sigma_y^2}, \sigma_x = \frac{\lambda}{1+\lambda}, \sigma_y = \frac{\tan \alpha}{1+\lambda} \tag{12}$$

where F_x and F_y are the modified longitudinal and lateral forces.

Based on the corrected tire model, and assuming that the vertical load F_z is 4 kN, the road friction coefficient is 1.0; the relationships of the longitudinal force and the slip ratio under different wheel slip angles and the lateral force and slip angle under different slip ratios are depicted in Fig. 2.

Because the estimation of road friction under driving and braking conditions is based on the driving wheels and the individual four wheels, it is necessary to describe the tire dynamics model. Since the rolling resistance moment generated by the elastic hysteresis of the tire is far too small compared to the other forces and torques, it is neglected in the model, though it is considered in the code used for the vehicle control. All the forces and torques related to the tire dynamics under combined slip conditions are briefly depicted in Fig. 3.

The rolling motion equation of the wheel is

$$J_w\dot{\omega} = T_t - T_b - F_x R \tag{13}$$
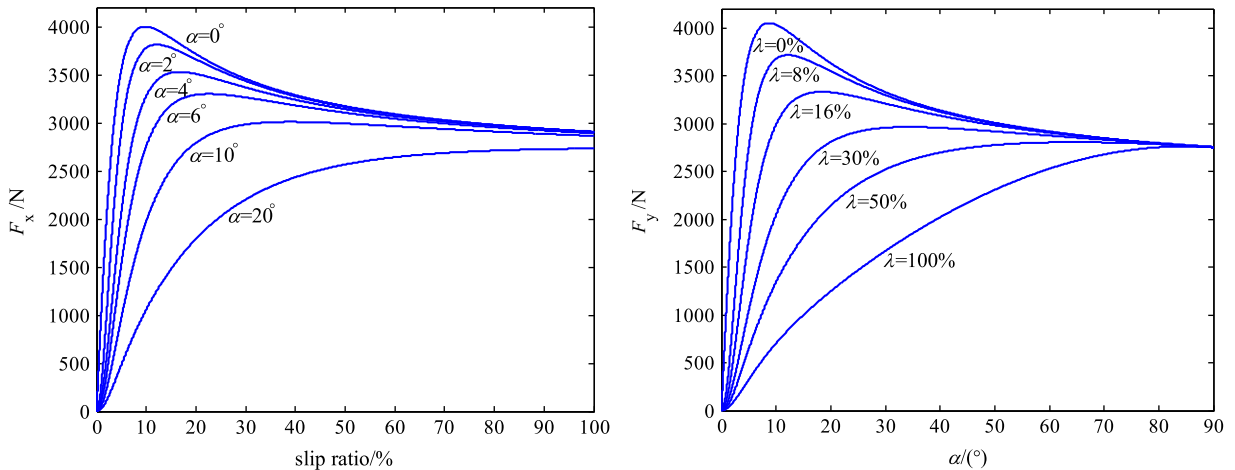
Fig. 2. The relationships of the longitudinal force and the slip ratio under different wheel slip angles, the lateral force and slip angle under different slip ratios (left: $F_x-\lambda$, right: $F_y-\alpha$).
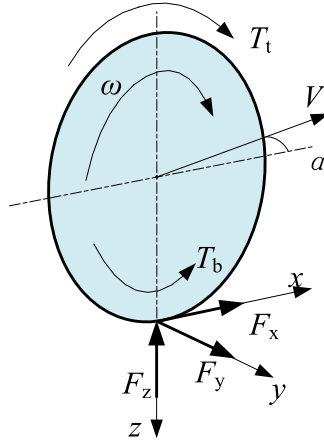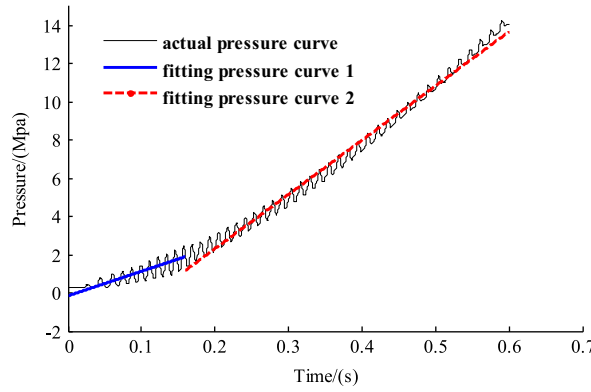
Fig. 3. The tire dynamics model.

Fig. 4. The pressure increasing characteristics.

where J_w is the inertia moment and R is the radius, which differs for the front and rear wheels. T_b is the braking torque on the wheels, which may be calculated using the estimated wheel cylinder pressure, which is presented in the next part. T_t is the driving torque from the engine; it may be computed using the engine torque T_e, which can be obtained directly from the engine management system. Therefore, the driving torque of the wheels may be expressed as follows:

$$T_t = \frac{1}{2}\eta_e i_g i_0 T_e \tag{14}$$

where η_e is the transmission efficiency of the engine; i_g and i_0 are, respectively the gear ratio and transmission ratio.

2.3. Brake pressure estimation model

To realize the control of the electronic stability control (ESC) system, active pressure intervention on wheels is needed. Since many vehicles are not equipped with pressure sensors, the pressure might be estimated during controlling. To estimate the pressure precisely, the Electronic Control Unit (ECU) calculates the target pressure on different road conditions; then a resembling Pulse Width Modulation (PWM) method is utilized; that is, finding pressure increasing or decreasing over one control period time by actuating the solenoid valves and the motor, while holding the pressure static, which is just like the modulation of the duty cycle.

The rate of pressure increase differs at different pressure levels; thus a piecewise fitting method is used, which is shown in Fig. 4. According to the pressure adjustment test there are three pressure increasing or decreasing modes, $u_{i,100}$, $u_{i,60}$, $u_{i,30}$, which means the actuator increases or decreases the pressure; for 30%, 60% and 100% time of the control period, and $i = 1, 2$ corresponding to two different pressure levels. The mode selection is shown in Fig. 5, where P_s is the piecewise point of the pressure. u_{inc} and u_{dec} are the increasing and decreasing rates respectively, e_p is the error of the target pressure P_{tar} and estimated pressure P_{est}, P_{est}^{k-1} and P_{est}^{k} are the estimated pressure for last period and this period. The related equations showing the calculation process of P_{est} with the signal for increasing or decreasing the pressure from the ECU
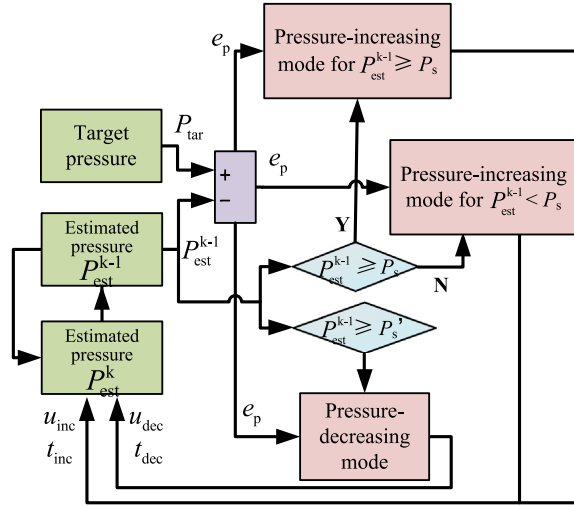
Fig. 5. The flowing diagram of the pressure increasing or decreasing time selection.

are listed as

$$e_p = \text{sign}\{P_{tar} - P_{est}\} \cdot (P_{tar} - P_{est}),$$

$$\begin{cases} u_{inc} = u_{i,100}, t_{inc} = 1 \cdot T_0 & u_{i,100} \cdot T_0 < e_p \\ u_{inc} = u_{i,60}, t_{inc} = 0.6 \cdot T_0 & u_{i,60} \cdot T_0 < e_p < u_{i,100} \cdot T_0 \\ u_{inc} = u_{i,30}, t_{inc} = 0.3 \cdot T_0 & u_{i,30} \cdot T_0 < e_p < u_{i,60} \cdot T_0 \\ u_{inc} = 0, t_{inc} = 0 & e_p < u_{i,30} \cdot T_0 \end{cases},$$

$$P_{est} = \sum T_0 \cdot u^{k-1} \tag{15}$$

where P_{est} is the estimated pressure, T_0 is the control period, and u^{k-1} is the adjusting rate of pressure in the last period. In addition, u^{k-1} is zero when the last pressure state is pressure-holding.

Besides, for the regular high-intensity braking conditions used in ABS runs, the hydraulic model proposed by Li et al. [25] is adopted in this paper. Since the wheel cylinder pressure is known, the braking torque to the wheels can be calculated as follows:

$$T_b = 2\mu' R_e A_{we} \eta P_{est} \tag{16}$$

where μ' is the friction coefficient of the brake pad, R_e is the equivalent radius of the brake plate, A_{we} is the wheel cylinder cross-sectional area, and η is the brake efficiency.

3. Signal fusion method

When running on the road, because of the complex maneuvering operations, the vehicle may not just run in one single condition such as driving, braking or steering only; on the contrary it may be involved with several situations, such as driving and steering or combined braking and steering conditions. As depicted in Fig. 6, the different maneuvering conditions may match the three areas generally.

Area I, which refers to the left first rectangle area in Fig. 6, corresponds to the condition with large steering only, where the friction coefficient mainly depends on the lateral friction; this is reflected in the figure where the lateral friction coefficient is big and the longitudinal one is extremely small. Area II, which refers to the middle area, represents the condition of driving and steering or braking and steering together, where the longitudinal and lateral frictions may both be taken into account to get the comprehensive one since both the longitudinal and lateral friction coefficients are considerable as shown in Fig. 6. In Area III, which is the right area, the lateral friction decreases rapidly, while the longitudinal friction is much more stable around a similar reference value, which means the longitudinal one dominates the road friction, that is, corresponding to the condition with driving or braking only.

As for the combined slip conditions the relationship between the normalized longitudinal and lateral forces may be described combining with the adhesion ellipse, which is shown as Fig. 7. From point 1 to 2 the vehicle is under high-intensity braking condition maybe with a very small slip angle, and the road friction heavily supplies the longitudinal force; this is similar from point 5 to 6 but under a strong-power driving condition. From point 3 to 4 the vehicle is under extremely large steering condition, where the road friction supplies the lateral force large. Besides, there are two more situations of the combined slip condition, such as point A, where the tire drops into the critical region; there the road friction may be
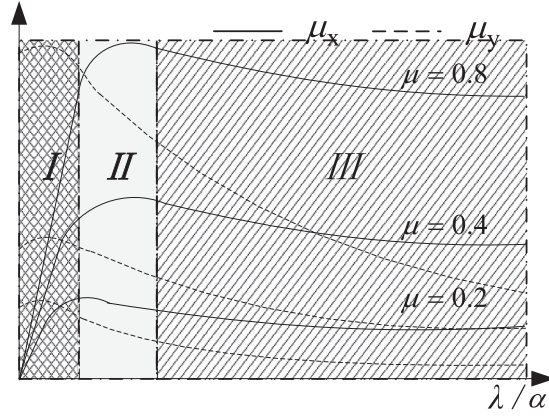
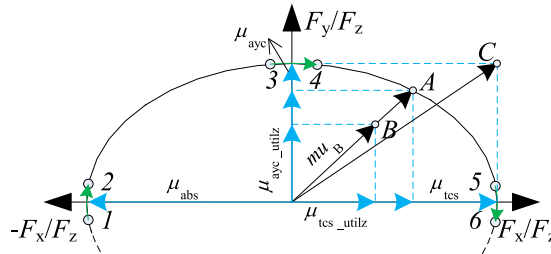**Fig. 6.** The areas matched to different maneuvering conditions.

Fig. 7. The relationship between F_x and F_y under combined slip conditions.

calculated using the utilized longitudinal and lateral frictions, which can be expressed as

$$mu = \sqrt{(F_x/F_z)^2 + (F_y/F_z)^2} \tag{17}$$

where mu is the road friction obtained using the utilized longitudinal and lateral frictions. And for point B the friction calculated by (17) can be less than the real one as seen obviously in Fig. 7; the calculated friction is mu_B, and the utilized ones are μ_{ayc_utilz} and μ_{tcs_utilz}; the real one should be the same as that at point A in the critical region as shown in Fig. 7. Thus, the method computed simply by Eq. (17) is not convenient for all kinds of situations.

However, the real road friction μ_{ayc} estimated through the vehicle characteristic during large steering can be obtained in this paper; besides, the complex maneuvering operations and the uncertain aspects of the road may also affect the estimation method of obtaining a stable and accurate friction coefficient; thus the μ_{ayc}, μ_{abs} and μ_{tcs} are used to calculate the road friction, where μ_{abs} and μ_{tcs} are, respectively the longitudinal road frictions under ABS and TCS runs as shown in Fig. 7. A method called signal fusion which combines the estimated μ_{ayc}, μ_{abs} and μ_{tcs} is proposed in this paper to make full use of the available signals to calculate the comprehensive road friction to make it as accurate and stable as possible. The architecture of the method may be expressed as shown in Fig. 8.

Considering that the fusion method using the computing way proposed by Eq. (17) may lead to a wrong value which may exceed the boundary of the adhesion ellipse, shown as point C in Fig. 7, and also the computation ability of the micro-computer, the signal fusion method is simplified by introducing certainty factors to obtain the comprehensive road friction, which may be expressed as

$$mu_{comp} = \frac{k_1 \cdot \mu_{abs} + k_2 \cdot \mu_{tcs} + k_3 \cdot \mu_{ayc}}{k_1 + k_2 + k_3} \tag{18}$$

where mu_{comp} is the estimated comprehensive road friction, k_1, k_2, k_3 are the certainty factors of μ_{abs}, μ_{tcs} and μ_{ayc} respectively. Since the slip angle and slip ratio of each wheel reflect the lateral and longitudinal characteristics of the wheels, they may be utilized to express the certainty factors of the lateral and longitudinal road frictions respectively. In addition, the longitudinal and lateral accelerations reflecting the characteristics of the vehicle are introduced as well to correct the certainty factors, which is shown in Fig. 8

$$k_i = \tau \cdot f_1(\lambda_j, \alpha_j) + (1 - \tau) \cdot f_2(a_x, a_y) \tag{19}$$

$$f_1(\lambda_j, \alpha_j) = \frac{|\lambda_j|}{\sqrt{\lambda_j^2 + \alpha_j^2}}, f_2(a_x, a_y) = \frac{|a_x|}{\sqrt{a_x^2 + a_y^2}} \tag{20}$$

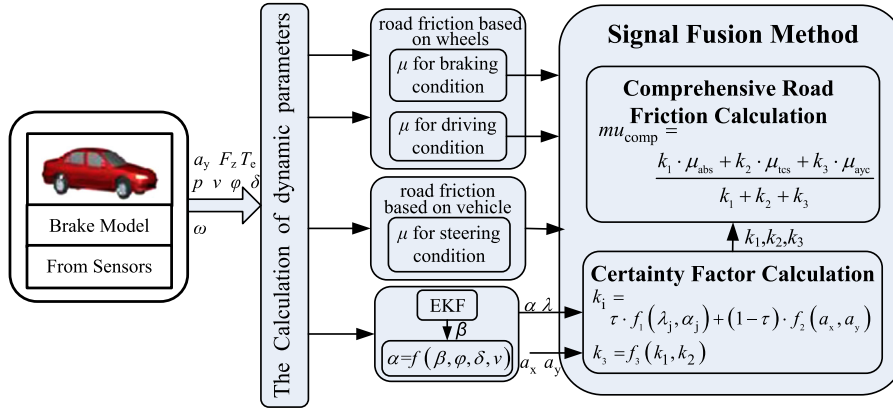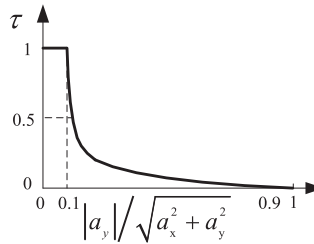**Fig. 8.** The signal fusion method structure.

Fig. 9. The weight coefficient decided by the wheel.
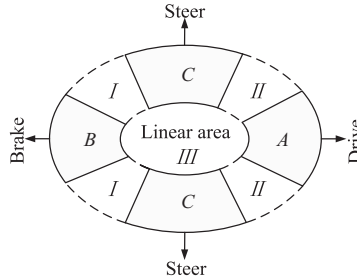

Fig. 10. Strategy under complex maneuvering operations.

where k_i is the certainty factor of braking condition for ABS or driving condition for TCS, corresponding to $i=1$ or 2, j represents the controlled wheel of the four wheels, and τ is the weight coefficient of $f_1(\lambda, \alpha)$ part decided by the wheel; while $f_2(a_x, a_y)$ part is decided by the vehicle, τ may be obtained through Fig. 9. From the figure, τ is decided by the lateral characteristic of the vehicle; there is a rapid decrease from value 1 because when the lateral characteristic is obvious the $f_2(a_x, a_y)$ part of k_i weighs more since the vehicle has huge inertia compared to the wheel, which means it may reflect the characteristic more robustly, while the wheels' longitudinal and lateral characteristics are extremely unstable caused by the noise through contact of the tire and road. Besides, what should be noticed is that since the driving and braking conditions are two opposite operations, k_1 or k_2 is known to be 0 once k_2 or k_1 is obtained, respectively. Thus, the certainty factor k_i reflects the compromise of the part decided by the vehicle and the part decided by the wheel which are both related to the longitudinal and lateral characteristics heavily in estimating the road friction.

The functions $f_1(\lambda, \alpha)$ and $f_2(a_x, a_y)$ are constructed by normalized λ, α and a_x, a_y, and there may be many other ways to construct the functions. Then, the certainty factor k_3 induced by the AYC runs for a complex maneuvering operation may be acquired as follows:

$$k_3 = 1 - k_1 - k_2 \tag{21}$$

In summary the estimation strategy of the signal fusion method under complex maneuvering operations discussed above may be shown as in Fig. 10, where areas A, B, C are driving, braking and steering conditions respectively, and areas I and II are the conditions of braking and steering together and driving and steering together, while area III is the stable condition when the dynamics control system has not been activated yet, which means the estimation of the road friction affects nothing, where the road friction is set to the original value. To summarize, the final comprehensive road friction may be

expressed as

$$mu_{comp} = \begin{cases} \mu_0 & vehicle \in III \\ \mu_{abs} & vehicle \in B \\ \mu_{tcs} & vehicle \in A \\ \mu_{ayc} & vehicle \in C \\ \frac{k_1 \cdot \mu_{abs} + k_3 \cdot \mu_{ayc}}{k_1 + k_3} & vehicle \in I \\ \frac{k_2 \cdot \mu_{tcs} + k_3 \cdot \mu_{ayc}}{k_2 + k_3} & vehicle \in II \end{cases} \tag{22}$$

4. Friction estimation for ABS/TCS/AYC

4.1. Road friction estimation method under ABS runs

When the vehicle encounters an emergency during high-speed driving, it may need to stop in very short time with a high-intensity braking, which may find interference by ABS control for some steering ability. Since the tires may move into a nonlinear region and the accurate dynamic states of the vehicle and tires may not be obtained easily, it may be a little hard and inconvenient for experimental vehicle test using the various control methods mentioned by a large number of papers just through simulation.

In this paper a converse method is proposed to estimate the road friction based on the relationship between the utilized friction and the slip ratio of the braking wheel, as shown in Fig. 11, where from the information for one specific slip ratio an utilized friction coefficient equaling the reference one, which is shown as the dashed lines, may be obviously acquired. Besides, for different roads, the specific slip ratios are generally close to each other, and then the reference friction may be obtained by setting a range around this specific slip ratio. For the slip ratios which are much bigger than the specific one, a constant certainty factor may be set since the utilized friction is relatively stable.

In order to get the utilized friction coefficient, the longitudinal force and the vertical force should be calculated first, which may be obtained by Eqs. (13) and (10). Hence, the utilized and the final estimated road friction may be expressed as follows:

$$\mu_{utilz} = \frac{F_x}{F_z}, \mu_{abs} = \begin{cases} \mu_0 & \lambda < \lambda_1 \\ \mu_{utilz} & \lambda_1 \leq \lambda \leq \lambda_2 \\ \mu_{utilz} \cdot k_{bliv1} & \lambda > \lambda_2 \end{cases} \tag{23}$$

where μ_{utilz} is the utilized friction coefficient, μ_0 is the set original value of friction coefficient and k_{bliv1} is the constant certainty factor.

4.2. Road friction prediction method under TCS runs

When driven on a low friction road, the driving wheels may skid easily due to the large output engine torque. In order to realize the TCS control accurately, and improve the vehicle's acceleration performance and stability, the road friction should be estimated stably to some extent in satisfying the controlling requirements.
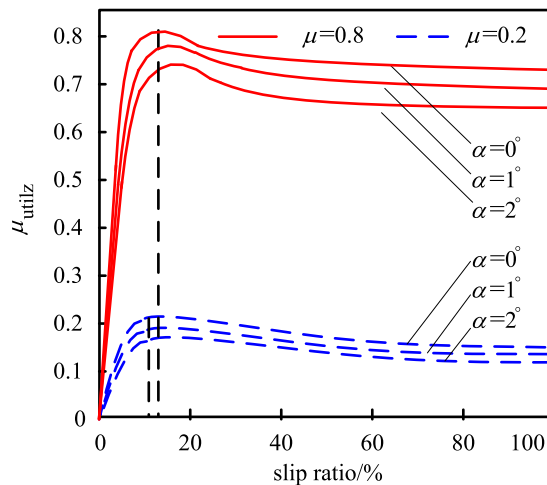

Fig. 11. The relationship between the utilized friction coefficient and the slip ratio of the braking wheel.

A method using the tire dynamics characteristics of driving wheels is proposed in this paper; the method is relatively easy of low-cost and viable, which makes it appropriate to utilize in experimental control. According to the tire dynamics equation which is shown as follows, the longitudinal force can be obtained; then the utilized road friction can be calculated with the vertical force:

$$F_x = \frac{T_t - J_w \dot{\omega} - T_b}{R} - F_f \tag{24}$$

where F_f is the resistance force of each driving wheel.

However, the relationship between the utilized road friction and the slip ratio of each driving wheel and what has been discussed before in the ABS runs part may be used for the friction estimation of the TCS controller. To judge the extent to which the utilized road friction can be trusted, a certainty factor is introduced; then the road friction may be calculated as

$$\mu_{tcs} = \frac{\mu_{utilz}}{k_{bliv2}} \tag{25}$$

where k_{bliv2} is the certainty factor.

In order to get the value of the certainty factor, the fuzzy logic control would be adopted considering the relationship between the slip ratio and the certainty factor. Apparently, the smaller the slip ratio, the lower the extent of trust; it is high for very large slip ratios, and there is a medium slip ratio corresponding to the highest extent of trust. Thus the fuzzy logic model is a single input and single output system, where the input state is the slip ratio of each driving wheel; and the output state is the certainty factor. Fig. 12 shows the architecture of the fuzzy logic observer, which consists of four steps [26].

1. *Step 1: Fuzzification.* This step generates the fuzzy sets and the variable universes of the input and output states. The variable universe of the input state λ is set as [0 0.6], the upper limit is set to be 0.6 because when λ is bigger than 0.6, it becomes stable without changing too much. The variable universe is divided into eight fuzzy sets using suitable linguistic variables, as shown in Table 2; the fuzzy sets can be defined as

   $$\{\lambda\} = \{ES, VS, S, MS, M, MB, B, VB\}$$

   and the variable universe of the output state k_{bliv2}, which is [0.5 1], is also divided into eight fuzzy sets, which can be defined asshown below in Table 3. The lower limit is set to be 0.5 because the difference of the utilized friction on different roads is not obvious to distinguish when the slip ratio is too small.

   $$\{k_{bliv2}\} = \{EL, VL, L, ML, M, MH, H, VH\}$$

2. *Step 2: Fuzzy decision process.* The fuzzy rules are the most important part of the entire method, which affect the output results crucially. They are set in this step based on the theoretical knowledge and extensive ground test results. The fuzzy rules can be described as listed below:

   If λ belongs to ES, then k_{bliv2} belongs to EL.
   If λ belongs to VS, then k_{bliv2} belongs to M.
   If λ belongs to S, then k_{bliv2} belongs to VH.
   If λ belongs to MS, then k_{bliv2} belongs to VH.
   If λ belongs to M, then k_{bliv2} belongs to H.
   If λ belongs to MB, then k_{bliv2} belongs to MH.
   If λ belongs to B, then k_{bliv2} belongs to MH.
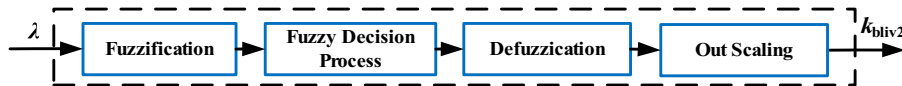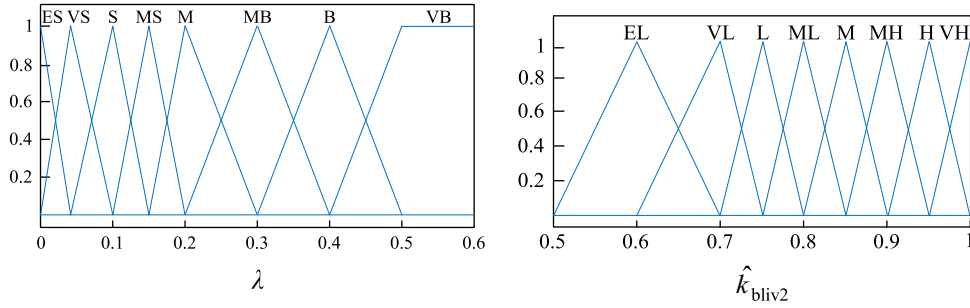   If λ belongs to VB, then k_{bliv2} belongs to M.

Fig. 12. Fuzzy logic method for the certainty factor.

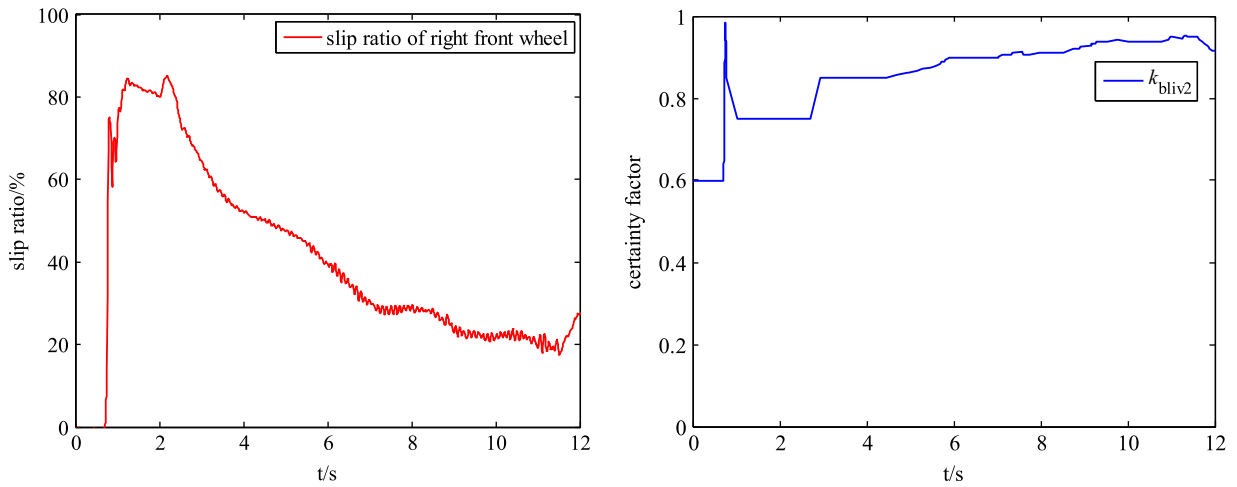**Table 2**
Linguistic terms of λ.

ES	Extremely small
VS	Very small
S	Small
MS	Medium small
M	Medium
MB	Medium big
B	Big
VB	Very big

Table 3
Linguistic terms of k_{bliv2}.

EL	Extremely low
VL	Very low
L	Low
ML	Medium low
M	Medium
MH	Medium high
H	High
VH	Very high

Fig. 13. Membership function for λ and k_{bliv2}.

Fig. 14. The example from winter test to verify the fuzzy logic method (left: the input state λ, right: the output state k_{bliv2}).

3. *Step 3: Defuzzification.* In this step, the fuzzy sets of the output state with the specific given inputs may be obtained by the fuzzy rules listed in step 2 using the popular Mamdani method [27]. To transfer the fuzzy values to clear ones, a centroid defuzzifier is adopted. The behaviors of the slip ratio and the certainty factor are illustrated in Fig. 13.

4. *Step 4: output scaling.* The output $\hat{k}_{bliv2}$ is scaled to map the certainty factor k_{bliv2}; the scaling factor may be adjusted through calibration test.

An example is shown in Fig. 14, which gives a data array from the winter test on icy road during an acceleration condition from static state, inputting the calculated slip ratio, and the output is the certainty factor. According to the calculated certainty factor, the road friction for TCS runs may be obtained using Eq. (25).

4.3. Road friction prediction method under AYC runs

When the vehicle is under a steering maneuvering, with the increasing of the vehicle yaw rate and slip angle, it may enter the critical instability region and lose control. Thus, the AYC system should be activated immediately before the
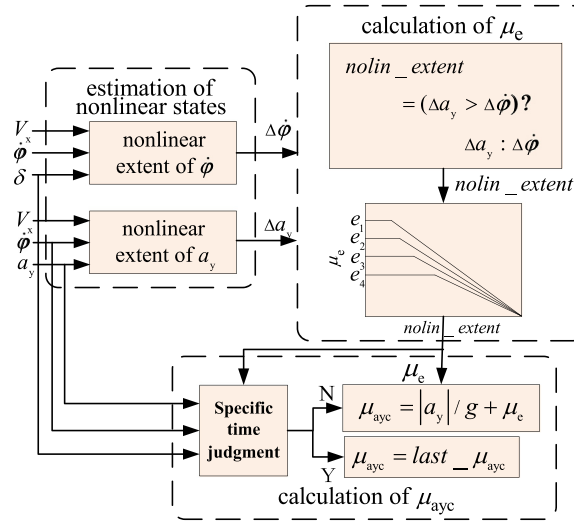
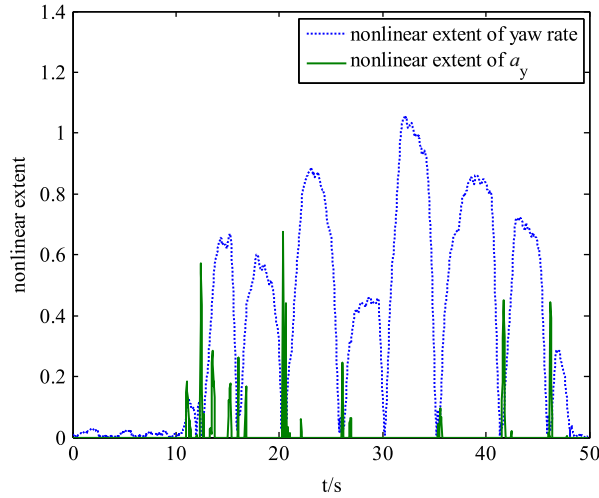**Fig. 15.** The estimation method of the vehicle lateral road friction.

Fig. 16. The nonlinear extents to obtain the compensative error for the friction coefficient.

vehicle drops into this region. To realize this, the control states such as the road friction should be estimated precisely and in time to ensure the control performance of the AYC system and thus the driver's and passengers' safety.

When driven on plain road, the lateral acceleration is proportional to the lateral tire force; specifically, the road friction is similarly equal to the measured lateral acceleration a_y divided by the gravity acceleration when the vehicle runs into the unstable area [28].

Based on the method proposed in [28], the nonlinear extent of the yaw rate $\dot{\varphi}$ was used to obtain the error of the friction μ_e which may compensate the detected lateral acceleration in estimating the road friction under steering conditions. This paper adds one more nonlinear extent of a_y reflecting the understeer condition to obtain the error since the nonlinear extent of $\dot{\varphi}$ reflects the oversteer conditions only. Thus the improved vehicle lateral friction estimation method may be shown as in Fig. 15, where μ_{e0} is the original value of μ_e, and the two nonlinear extents may be expressed as follows:

$$\Delta\dot{\varphi} = \left\{ 1 + \left(\frac{V_x}{V_c}\right)^2 \right\} \frac{(\dot{\varphi}_{ref} - \dot{\varphi})l}{V_x} \frac{|\dot{\varphi}|}{\dot{\varphi}}, \Delta a_y = |V_x \cdot \dot{\varphi} - a_y| \qquad (26)$$

where $\Delta\dot{\varphi}$ and Δa_y are the nonlinear extents of the yaw rate and the lateral acceleration respectively, and V_c is the characteristic speed of the vehicle, $\dot{\varphi}_{ref}$ is the nominal yaw rate, which may be calculated as

$$\dot{\varphi}_{ref} = \frac{V_x}{l} \frac{\delta}{1 + (V_x/V_c)^2} \qquad (27)$$

Fig. 16 shows the necessity to add the nonlinear extent of a_y, which may reflects the nonlinear extent of the tire forces in understeer situations, while the nonlinear extent of $\dot{\varphi}$ could not.

The vehicle works very close to the unstable region with the increase of the nonlinear extents, which means a_y dominates the road friction largely. Thus, between the nonlinear extents of the yaw rate and the lateral acceleration, the bigger one is chosen as the final value. Then, the road friction may be expressed as

$$\mu_{ayc} = |a_y|/g + \mu_e \tag{28}$$

where μ_{ayc} is the road friction under AYC runs, g is the gravity acceleration, and μ_e is the compensative error of the road friction, which decreases as the nonlinear extent increases.

Considering the different friction coefficients of different roads, such as icy road, snowy road, rainy road, dry asphalt road, etc. the method proposed in this paper classifies μ_{e0} into different values according to the characteristics of the vehicle, which may reflect what kind of road the vehicle is running on generally, instead of using a stable value as in [28]. The product of the yaw rate and the longitudinal velocity given by $mu_{yawrate}$ is chosen to set the value of μ_{e0}, which is shown in Fig. 17.

In addition, because the method proposed in this paper is mainly used in real controller of Electronic Stability Program (ESP) for experimental vehicle test, there are too many uncertain factors during running on the road; thus, just the method described above may not be sufficient to guarantee the stability of the estimation; especially when the steering is near to
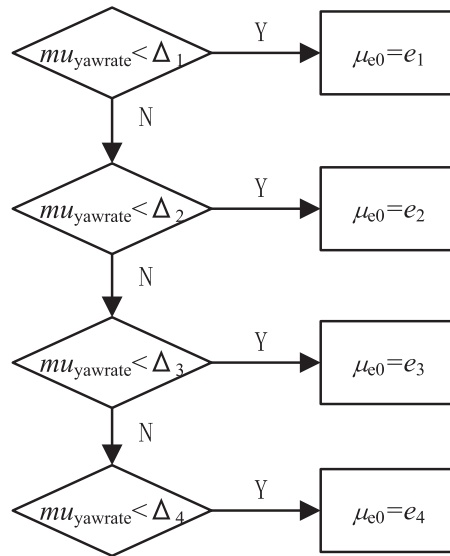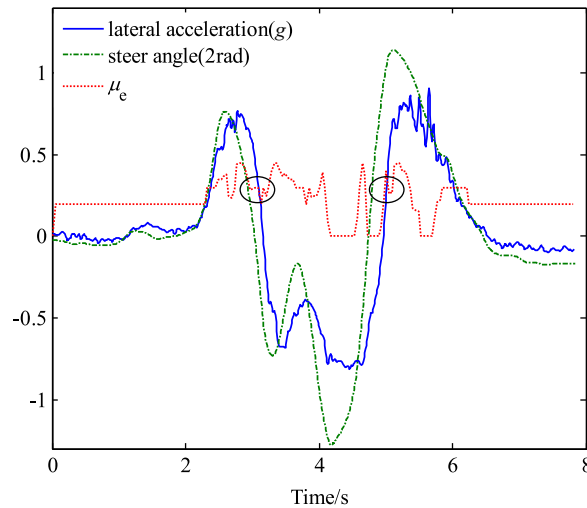

Fig. 17. The flow diagram of setting μ_{e0}.

Fig. 18. The characteristic states of the vehicle.

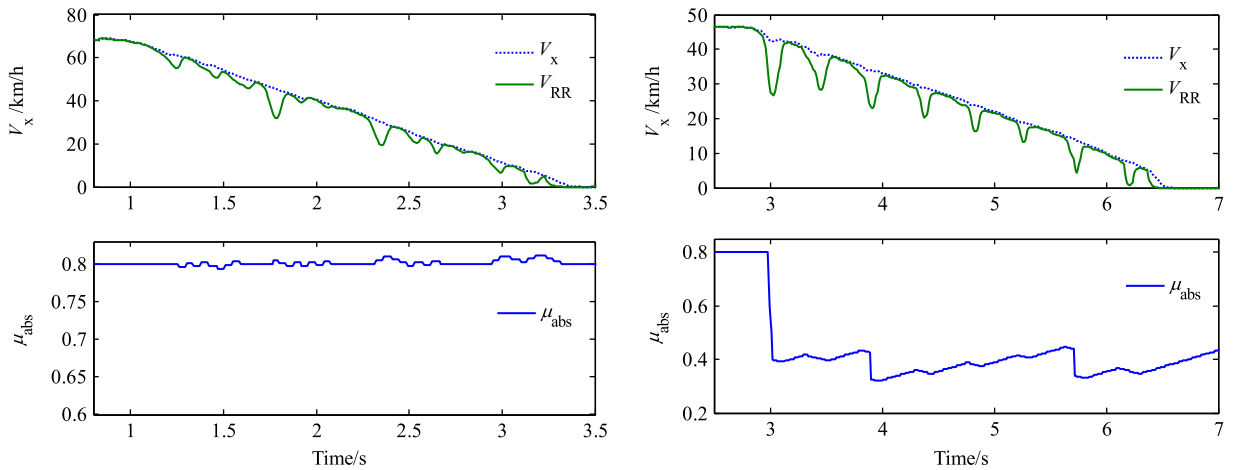**Fig. 19.** The tested vehicle and the test ground.

Fig. 20. The test results for high-intensity braking. (a) The results on dry asphalt road and (b) the results on the road covering plastic floor with sprinkled soap water.

zero the lateral acceleration a_y is extremely small, and the compensative error μ_e obtained through the nonlinear extent is not always that perfect, it may be small, as shown in Fig. 18, plotted from a data array of vehicle test on asphalt road, which results in a lower estimation than the real road friction; this could be recognized at 3.1 s, 4.9 s, etc.

In order to avoid this kind of times mentioned before to ensure the stability of the estimation method the road friction is not estimated during these specific periods such as those discussed in Fig. 18, where the estimated value in previous period stays. The sign of these times may be expressed by the steering angle; considering the lag between the lateral acceleration, the yaw rate and the steer angle, some research have been done to reduce the time delay [29].

5. Test results

A passenger car from Brilliance-Auto® Company equipped with the vehicle dynamics control systems with the estimating method proposed was used in the test to verify the feasibility. The tests were demonstrated on dry asphalt road, packed-snow road and icy road with maneuvering operations such as double-lane-change test, slalom test, steady circle test, etc. The tested car and the test ground are shown in Fig. 19.

5.1. High-intensity braking test for ABS runs

Fig. 20 shows the test and estimated results with high-intensity braking on different roads. For the maneuvers of braking to stop at 70 km/h in Fig. 20(a) and at 45 km/h in Fig. 20(b) without steering the comprehensive friction mainly depends on the value estimated by ABS control method; this figure shows the reference longitudinal velocity of the vehicle and wheel speed of the rear right wheel from the sensor directly, and the filtered estimated road friction when ABS is activated. Fig. 20(a) shows the test result on dry asphalt road; the estimated result fluctuates around 0.8 slightly; Fig. 20(b) shows the test results on the road covering plastic floor with sprinkled soap water, which is to simulate the low friction road, with an estimated road friction around 0.38. And the test results verified the accuracy and feasibility of the method for the control system.
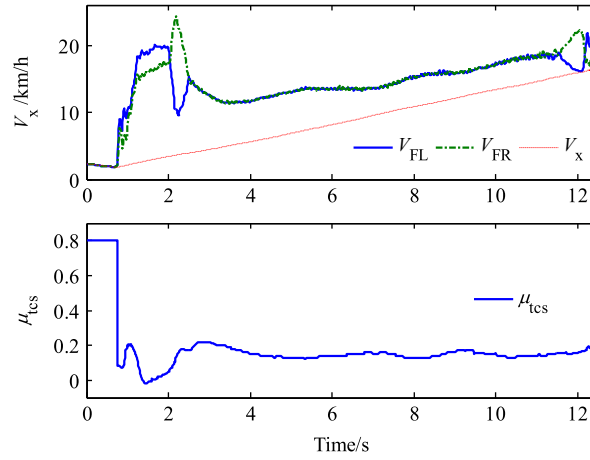
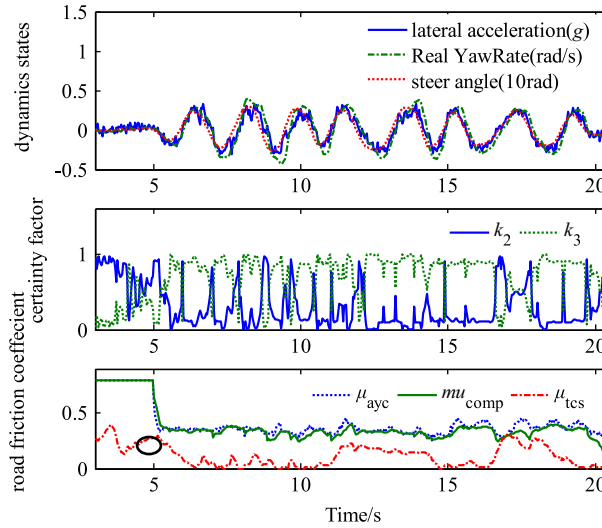**Fig. 21.** The test result on icy road for TCS runs.

Fig. 22. The slalom test result on packed-snow road.

5.2. Driving test on icy road for TCS runs

Fig. 21 shows the test result of driving condition with an input of high throttle percentage on icy road. From the result it is shown that the driving wheels skid too much at first because of the high engine power and the low road friction, but the controller controls the slip ratio of the driving wheels at a relatively stable value by recognizing the road friction in time. In the braking condition the road friction is used mainly to supply the longitudinal force, which means that the estimated road friction for TCS runs decides the comprehensive one heavily, which is about 0.18 approximately from the figure. And it is very close to the adhesion coefficient of icy road.

5.3. Slalom test for complex maneuvering operations

Fig. 22 shows the test result under slalom test on packed-snow road. Since the road friction is lower compared to the dry asphalt road the driving wheels may easily skid sometimes in steering conditions, which means the TCS control system and the AYC control system should act at the same time to ensure the vehicle's stability and the passengers' safety in any situation.

From Fig. 22, it is obvious that, even on snowy road, the comprehensive road friction is still largely decided by the lateral friction of the road during a steering condition, however it combines the road friction coefficient estimated by TCS system when the certainty factor k_2 is bigger, which means the system enters TCS control as depicted in the figure. In addition there are also some time points when the road frictions estimated by TCS system and AYC system combine together to yield a comprehensive one where both the certainty factors are not that big such as at time 7 s, 9 s, 9.5 s, etc. which is because
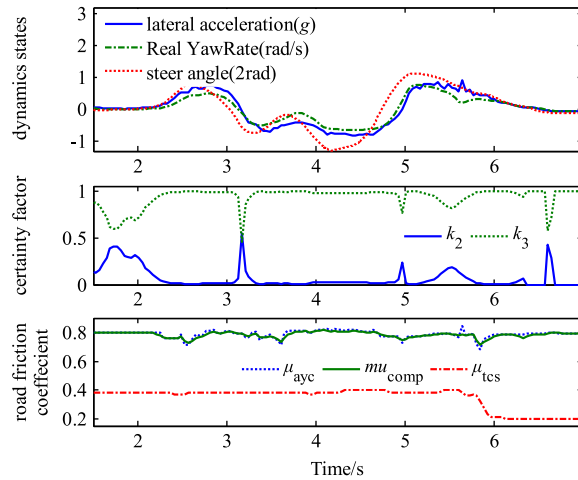
Fig. 23. The result of the double lane change test on dry asphalt road.

when the steering wheel is back to zero, the lateral acceleration also tends to decrease to zero, then the lateral acceleration decreases when the longitudinal acceleration increases, which changes the sign of the road friction estimated by lateral and longitudinal directions, namely, μ_{ayc} and μ_{tcs}. Thus, the estimated comprehensive road friction may drop to extremely low value at these times. To avoid this, the road friction is not estimated but is made to be equal to the lateral one which is μ_{ayc} directly.

The result shows that the comprehensive road friction coefficient estimated is around 0.33, which agrees with the real value of the packed-snow road which is 0.3; this means the estimation method can satisfy the accuracy of the control system. Besides, the road friction is recognized immediately when the steering operation is maneuvered but before the vehicle drops into an unstable area at around 5 s, which shows the real-time demands.

5.4. Double lane change test for complex maneuvering operations

Fig. 23 is the result of the double lane change test, which is maneuvered on dry asphalt road. The operation includes driving and sudden steering. Because of the high friction between the tire and the road the driving wheels hardly skid even with a strong power to drive the vehicle, reflecting in the figure that the certainty factor k_2 which represents the believable extent of the longitudinal road friction, is very low all the time. According to the discussion above, only the AYC is activated of the vehicle dynamics control systems for most time, which means the weight of the estimated road friction for TCS is awfully low and extremely high for AYC for the signal fusion method proposed in this paper. Thus the comprehensive road friction is mainly decided by the lateral one, which results in the filtered value almost coinciding with μ_{ayc}; this conclusion is also obviously gained from the figure. However, at the time points like 3.2 s and 4.9 s, the lateral acceleration is near to zero, and the certainty factor k_2 can be large due to the lateral load transfer; however, the road friction is not estimated at these times to avoid this as discussed before.

The result shows that the estimated road friction coefficient is about 0.78 and this is close to 0.8, which is defined as the real value of the dry asphalt road.

5.5. Steady circle test for steering operations

Fig. 24 shows the steady circle test results with a firm radius which is 15 m and a firm throttle percentage on different roads, which are maneuvered on packed-snow road in Fig. 24(a) and on dry asphalt road in Fig. 24(b). Both of the estimated comprehensive road frictions are fused by the longitudinal and lateral ones which can be acknowledged directly from the results.

When the vehicle is tested on packed-snow road the lateral acceleration is always high compared to the longitudinal one, and the wheel slip angle is somewhat stable while the slip ratio can be high at some time points during the whole process, which results in a high value of the certainty factor k_3 most of the time and relatively low when the slip ratio is high; this is opposite in case of k_2, corresponding to the weight of the estimated lateral friction μ_{ayc} and the longitudinal μ_{tcs} to obtain the comprehensive road friction; these can be seen in Fig. 24(a). The result shows that the comprehensive road friction coefficient is around 0.32 estimated by the signal fusion method, which is very similar to the real one.

As discussed above, the estimated comprehensive road friction on dry asphalt road is also a fusion of μ_{ayc} and μ_{tcs}; the control system entering the TCS control on high friction road is because while steering with a strong power the lateral acceleration of the vehicle is close to the friction limit between the road and tire, which results in an appreciable load
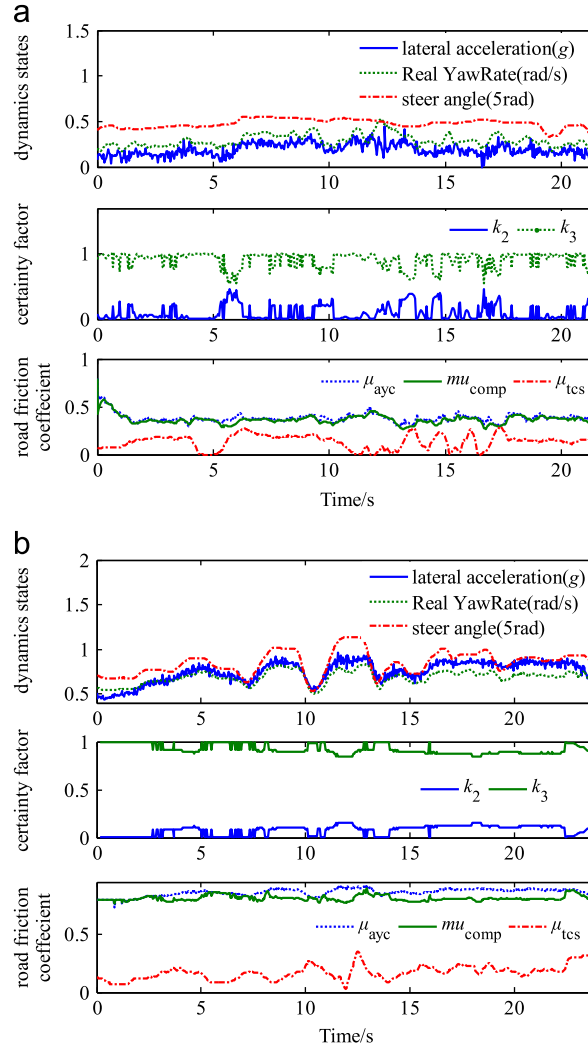
Fig. 24. The results of the steady circle test. (a) The results on packed-snow road and (b) the results on dry asphalt road.

transfer laterally. Then the inner wheel may skid very easily because of the centrifugal force. The estimated road friction coefficient is around 0.8 as shown in Fig. 24(b), reflecting the accuracy of the signal fusion method.

6. Conclusion

A comprehensive method with fusion of the valuable signals of the vehicle dynamics control system is proposed in this paper, to estimate the road friction with transient maneuvering conditions accurately and in real-time. Firstly, the road friction under relatively simple maneuvering operations can be estimated with viable methods for ABS, TCS and AYC runs; then the certainty factors are set based on the longitudinal and lateral accelerations, slip ratio of the wheel and the wheel slip angle. Thus, the comprehensive road friction coefficient is obtained with proper fusion for complex maneuvering operations. The real vehicle experimental tests were conducted on packed snow ground and dry concrete roads; the test results showed that the road friction estimated by the signal fusion method can satisfy the controlling demands, which verified the feasibility properly.

The basic state values such as the slip ratio λ and slip angle α can affect the accuracy of the estimated road friction directly. However, in the complicated combined slip operations such as steering–braking operation, the estimated errors of the basic states might be increased and might decrease the accuracy of any estimation method. Thus, the proposed method should be calibrated for all types of real vehicle test and improved.

Acknowledgments

References

[1] Dongpu Cao, Xubin Song, Mehdi Ahmadian, Editors' perspectives: road vehicle suspension design, dynamics, and control, Veh. Syst. Dyn. 49 (1–2) (2011) 3–28.

[2] Weichao Sun, Huijun Gao, et al., Finite frequency H_∞ control for vehicle active suspension systems, IEEE Trans. Control Syst. Technol. 19 (2) (2011) 416–422.

[3] Alireza Pazooki, Subhash Rakheja, Dongpu Cao, Modeling and validation of off-road vehicle ride dynamics, Mech. Syst. Signal Process. 28 (2012) 679–695.

[4] Dongpu Cao, Subhash Rakheja, Chunyi Su, Roll- and pitch-plane coupled hydro-pneumatic suspension, Veh. Syst. Dyn. 48 (3) (2010) 361–386.

[5] C. Ahn, H. Peng, H.E. Tseng, Robust estimation of road friction coefficient using lateral and longitudinal vehicle dynamics, Veh. Syst. Dyn. 50 (6) (2012) 961–985.

[6] S. Müller, M. Uchanski, J.K. Hedrick, Estimation of the maximum tire–road friction coefficient, J. Dyn. Syst. Meas. Control 125 (2003) 607–617.

[7] A.T. van Zanten, Bosch ESP system: 5 years of experience. SAE Paper 2000-01-1633, 2000.

[8] T. Bachmann, The importance of the integration of road, tire, and vehicle technologies, in: Proceedings of the FISITA 20th World Congress, 1995.

[9] U. Eichhorn, J. Roth, Prediction and monitoring of tire–road friction, in: Proceedings of the FISTA 24th Congress: Safety, the Vehicle, and the Road. Tech. Paper, vol. 2, 1992, pp. 67–74.

[10] B. Breuler, U. Eichhorn, J. Roth, Measurement of tire–road friction ahead of the car and inside the tire, in: Proceedings of the 92 International Symposium on Advanced Vehicle Control, AVEC, 1992, pp. 347–353.

[11] S. Yamazaki, O. Furukawa, T. Suzuki, Study on real time estimation of tire to road friction, Veh. Syst. Dyn. (Suppl (27)) (1997) S225–S233.

[12] A. Carcaterra, N. Roveri, Tire grip identification based on strain information: theory and simulations, Mech. Syst. Signal Process. 41 (1) (2013) 564–580.

[13] C. Lee, K. Hedrick, K. Yi, Real-time slip-based estimation of maximum tire–road friction coefficient, IEEE/ASME Trans. Mechatron. 9 (2) (2004) 454–458.

[14] R. Rajamani, G. Phanomchoeng, D. Piyabongkarn, Jae Y. Lew, Algorithms for real-time estimation of individual wheel tire–road friction coefficient, IEEE/ASME Trans. Mechatron. 17 (2012) 6.

[15] J.O. Hahn, R. Rajamani, L. Alexander, GPS-based real-time identification of tire–road friction coefficient, IEEE Trans. Control Syst. Technol. 10 (3) (2002) 331–343.

[16] S. Hong, C. Erdogan, K. Hedrick, F. Borrelli, Tire–road friction coefficient estimation based on tire sensors and lateral tire deflection: modelling, simulations and experiments, Veh. Syst. Dyn. 51 (5) (2013) 627–647.

[17] L.R. Ray, Nonlinear tire force estimation and road friction identification: simulation and experiments, Automatica 33 (1997) 1819–1833.

[18] D.L. Hall, J. Llinas, An introduction to multisensor data fusion, Proc. IEEE 85 (1) (1997) 6–23.

[19] H. Lee, Reliability indexed sensor fusion and its application to vehicle velocity estimation, J. Dyn. Syst., Meas., Control 128 (2) (2006) 236–243.

[20] L. Li, J. Song, L. Kong, Q. Huang, Vehicle velocity estimation in real time control for stability dynamic control, Proc. Inst. Mech. Eng., Part D: J. Automob. Eng. 10 (6) (2009) 675–685.

[21] K.T. Leung, J.F. Whidborne, D. Purdy, et al., Road vehicle state estimation using low-cost GPS/INS, Mech. Syst. Signal Process. 25 (6) (2011) 1988–2004.

[22] L. Li, J. Song, H. Li, et al., A variable structure adaptive extended Kalman filter for vehicle slip angle estimation, Int. J. Veh. Des. 56 (1) (2011) 161–185.

[23] S. Melzi, E. Sabbioni, On the vehicle sideslip angle estimation through neural networks: numerical and experimental results, Mech. Syst. Signal Process. 25 (6) (2011) 2005–2019.

[24] Y. Shibahata, K. Shimada, T. Tomari, The improvement of vehicle maneuverability by direct yaw moment control, Veh. Syst. Dyn. 22 (1993) 465–481.

[25] L. Li, J. Song, H.-Z. Li, D.-S. Shan, L. Kong, C.C. Yang, Comprehensive prediction method of road friction for vehicle dynamics control, Proc. Inst. Mech. Eng., Part D: J. Automob. Eng. 223 (8) (2009) 987–1002.

[26] B.L. Boada, M.J.L. Boada, V. Dı́az, Fuzzy logic applied to yaw moment control for vehicle stability, Veh. Syst. Dyn. 3 (2005) 753–770.

[27] F. Tahami, S. Farhangi, R. Kazemi, A fuzzy logic direct yaw-moment control system for all-wheel-drive electric vehicles, Veh. Syst. Dyn. 41 (3) (2004) 203–221.

[28] Y. Fukada, Slip-angle estimation for vehicle stability control, Veh. Syst. Dyn. 32 (4–5) (1999) 375–388.

[29] H.-J. Zhu, L. Li, M.-J. Jin, et al., Real-time yaw rate prediction based on nonlinear model and feedback compensation for vehicle dynamics control, Proc. Inst. Mech. Eng., Part D: J. Automob. Eng. 227 (10) (2013) 1431–1444.